

Linear phase-and-frequency-modulated photonic links using optical discriminators

J. M. Wyrwas,^{1,*} R. Peach,² S. Meredith,² C. Middleton,² M. S. Rasras,³ Kun-Yii Tu,³ M. P. Earnshaw,³ F. Pardo,³ M. A. Cappuzzo,³ E. Y. Chen,³ L. T. Gomez,³ F. Klemens,³ R. Keller,³ C. Bolle,³ L. Zhang,⁴ L. Buhl,⁴ M. C. Wu,¹ Y.K. Chen,³ and R. DeSalvo²

¹ Department of Electrical Engineering and Computer Sciences, University of California, Berkeley, CA 94720, USA

² Harris Corporation, MS 13-11A, P.O. Box 37, Melbourne, FL 32905-0037, USA

³ Bell Laboratories, Alcatel-Lucent, 600-700 Mountain Ave., Murray Hill, NJ 07974, USA

⁴ Bell Laboratories, Alcatel-Lucent, 791 Holmdel Road, Holmdel, NJ 07733, USA

jwyrwas@berkeley.edu

Abstract: We report our experimental results for linear analog optical links that use phase or frequency modulation and optical discrimination. The discriminators are based on two architectures: a cascaded MZI FIR lattice filter and a ring assisted MZI (RAMZI) IIR filter. For both types of discriminators, we demonstrate > 6 dB improvement in the link's third-order output intercept point (OIP3) over a MZM link. We show that the links have low second-order distortion when using balanced detection. Using high optical power, we demonstrate an OIP3 of 39.2 dBm. We also demonstrate 4.3dB improvement in signal compression.

©2012 Optical Society of America

OCIS codes: (060.2360) Fiber optic links and subsystems; (060.5060) Phase modulation; (060.5625) Radio frequency photonics; (070.6020) Signal processing; (130.3120) Integrated optics devices; (350.4010) Microwave.

References and links

1. Y. Li, R. Wang, A. Bhardwaj, S. Ristic, and J. Bowers, "High linearity InP-based phase modulators using a shallow quantum-well design," *IEEE Photon. Technol. Lett.* **22**(18), 1340–1342 (2010).
2. X. Xie, J. Khurgin, F. S. Choa, X. Yu, J. Cai, J. Yan, X. Ji, Y. Gu, Y. Fang, Y. Sun, G. Ru, and Z. Chen, "A model for optimization of the performance of frequency-modulated DFB semiconductor laser," *IEEE J. Quantum Electron.* **41**(4), 473–482 (2005).
3. S. E. Harris, E. O. Ammann, and I. C. Chang, "Optical network synthesis using birefringent crystals," *J. Opt. Soc. Am.* **54**(10), 1267–1278 (1964).
4. I. P. Kaminow, "Balanced optical discriminator," *Appl. Opt.* **3**(4), 507–510 (1964).
5. V. J. Urick, F. Bucholtz, P. S. Devgan, J. D. McKinney, and K. J. Williams, "Phase modulation with interferometric detection as an alternative to intensity modulation with direct detection for analog-photonic links," *IEEE Trans. Microw. Theory Tech.* **55**(9), 1978–1985 (2007).
6. W. Way, Y. Lo, T. Lee, and C. Lin, "Direct detection of closely spaced optical FM-FDM Gb/s microwave PSK signals," *IEEE Photon. Technol. Lett.* **3**(2), 176–178 (1991).
7. P. Driessen, T. Darcie, and J. Zhang, "Analysis of a class-B microwave-photonic link using optical frequency modulation," *J. Lightwave Technol.* **26**(15), 2740–2747 (2008).
8. X. Xie, J. Khurgin, J. Kang, and F.-S. Choa, "Ring-assisted frequency discriminator with improved linearity," *IEEE Photon. Technol. Lett.* **14**(8), 1136–1138 (2002).
9. D. Marpaung, C. Roeloffzen, A. Leinse, and M. Hoekman, "A photonic chip based frequency discriminator for a high performance microwave photonic link," *Opt. Express* **18**(26), 27359–27370 (2010).
10. C. H. Cox, "Distortion models and measures," in *Analog Optical Links: Theory and Practice* (Cambridge University Press, 2004), pp. 202–216.
11. J. M. Wyrwas and M. C. Wu, "Dynamic range of frequency modulated direct-detection analog fiber optic links," *J. Lightwave Technol.* **27**(24), 5552–5562 (2009).
12. K. Takiguchi, K. Jinguji, K. Okamoto, and Y. Ohmori, "Variable group-delay dispersion equalizer using lattice-form programmable optical filter on planar lightwave circuit," *IEEE J. Sel. Top. Quantum Electron.* **2**(2), 270–276 (1996).
13. M. S. Rasras, Y. K. Chen, K. Yii, M. P. Earnshaw, F. Pardo, M. A. Cappuzzo, E. Y. Chen, L. T. Gomez, F. Klemens, R. Keller, C. Bolle, L. Buhl, J. M. Wyrwas, M. C. Wu, R. Peach, C. Middleton, and R. DeSalvo, "A reconfigurable linear optical FM discriminator," *IEEE Photon. Technol. Lett.* **24**(20), 1856–1859 (2012).
14. J. M. Wyrwas and M. C. Wu, "High dynamic-range microwave photonic links using maximally linear FIR optical filters," in *Optical Fiber Communication Conference, OSA Technical Digest (CD)* (Optical Society of America, 2010), paper JWA43.

15. V. E. Houtsma, T. Hu, N. Weimann, R. Kopf, A. Tate, J. Frackoviak, R. Reyes, Y. Chen, and L. Zhang, "A 1 W linear high-power InP balanced uni-traveling carrier photodetector," in *37th European Conference and Exposition on Optical Communications*, OSA Technical Digest (CD) (Optical Society of America, 2011), paper Tu.3.LcSaleve.6.
-

1. Introduction

Microwave photonic links (MPLs) with low signal distortion are an essential component of high-performance microwave distribution and processing systems. Phase modulation (PM) is a promising modulation technique for MPLs because it is highly linear. Phase modulators based on the linear electro-optic effect, including those fabricated in lithium niobate, are intrinsically linear, and authors have also reported linear, integrable phase modulators fabricated in indium-phosphide [1]. The signal loss of MPLs is also an important factor for links and systems. Traditional intensity-modulated direct-detection (IMDD) links experience large signal-loss and result in low noise figures due to the low modulation efficiency of lithium niobate Mach Zehnder modulators (MZMs). On the other hand, frequency modulated (FM) lasers have been demonstrated with very high modulation efficiency [2]. PM and FM have favorable characteristics for linearity and gain in MPLs.

Although the modulation may be linear, distortion is introduced in the demodulation process. We have designed demodulators which use optical filters to convert the phase and frequency modulation into AM before detection at a photodetector. The filters are called phase and frequency discriminators. The demodulation process is called phase-modulation or frequency-modulation direct-detection (PM-DD or FM-DD), filter-slope detection, or interferometric detection. Authors have proposed various discriminator-filters to optimize the demodulation for low distortion, including birefringent crystals [3], asymmetrical Mach Zehnder interferometers (a-MZI) [4,5], Fabry-Perot filters [6], fiber Bragg gratings [7] and tunable integrated filters [8,9].

Using "complementary linear-field" discriminator filters, we believe we have demonstrated PM-DD and FM-DD links with the highest linearities which have been published thus far, as measured by third-order and second-order output-intercept points (OIP3 and OIP2) normalized to a fixed, photodetector-limited photocurrent. A variety of figures of merit are used in the field [10]. We use the output-intercept points as our figures of merit since they are independent of the laser noise and detector power handling, which can be optimized separately. Our discriminator filters are fabricated in a low-loss silica-on-silicon, planar-lightwave-circuits (PLC) process at Alcatel-Lucent Bell Laboratories. The linear-field filter transfer functions and low-loss fabrication technology are unique from previous published work [3–9]. We report link measurements using both a cascaded MZI FIR lattice filter and a ring assisted MZI (RAMZI) IIR filter, and with both PM and FM.

2. Link architecture

Figure 1 illustrates the architecture for the PM-DD and FM-DD links. Discriminators for FM-DD links can also be used to discriminate phase modulation because FM is identical to PM but with a modulation depth that is linearly dependent on modulation-frequency. In both links, the ideal transfer function of the optical filter is a linear ramp of field-transmission versus frequency offset from the optical carrier, which, we emphasize, is a quadratic ramp of power transmission. The ideal filters have linear phase. The power is split between two filters with complementary slope, and detected with a balanced photodetector. This complementary linear-field demodulation scheme was analyzed analytically in [11], but experimental results have not yet been reported. A single filter and detector has low third-order distortion, and the balanced detection cancels second-harmonics produced by squaring of the AM.

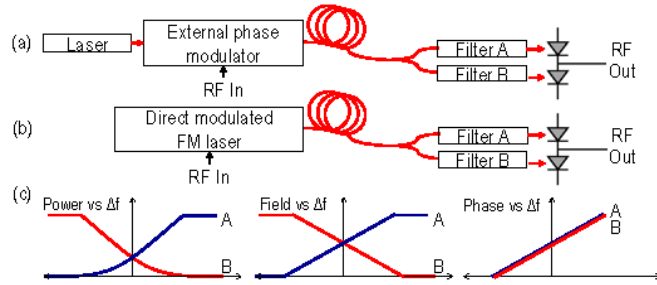


Fig. 1. (a) Diagram of a phase-modulated direct-detection photonic link (b) Diagram of a frequency-modulated direct-detection link (c) Desired amplitude and phase for the filters.

We implement the complementary linear-field filters using two different types of tunable PLC filters: a MZI FIR lattice filter and a ring assisted MZI (RAMZI) IIR filter. A single stage of each filter is illustrated in Fig. 2. These filters can be thermally tuned to implement arbitrary filter transfer functions. Our FIR filter is a sixth-order filter with 120 GHz free-spectral range. An N th order FIR lattice filter is composed of N a-MZIs (delay line interferometers), and $N + 1$ symmetrical MZIs (switches) to control the coupling into each branch. Up to tenth-order FIR lattice filters have been previously fabricated for dispersion compensation and gain equalization [12]. The RAMZI filter is an all pass ring resonator structure coupled to the delay arm of an MZI. We report on the physical design and fabrication, and tuning of this filter in [13], while the system measurement results are contained within this work.

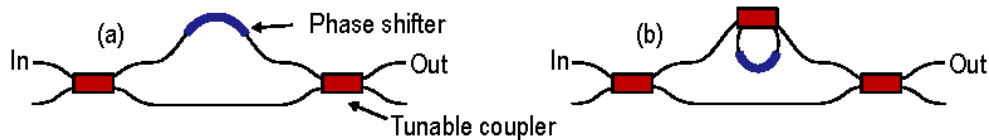


Fig. 2. (a) Filter stage for an FIR lattice filter (b) Filter stage for an IIR, RAMZI filter.

3. Characterization

The experimental system for a phase-modulated link measurement is illustrated in Fig. 3. A polarization tracker is used at the output of the ECTL, and, where possible, the optical paths are polarization maintaining fiber. Two tunable RF sources are combined to modulate a commercial lithium niobate phase modulator to perform two-tone distortion measurements. We use a personal-computer-based analog output card to generate bias currents for the heaters to tune the transfer function of the discriminator. The paths between the filters and balanced detectors are trimmed to match delay and attenuation. For the FM measurements, the tunable laser, polarization controller, and phase modulator are replaced with the directly modulated FM laser. The n th output-intercept points (OIPN) are defined by measuring the output power at the fundamental frequency and the N th order distortion products with the spectrum analyzer, taking an N th order polynomial interpolation of the product power until it intercepts with the fundamental power, and reporting that output power.

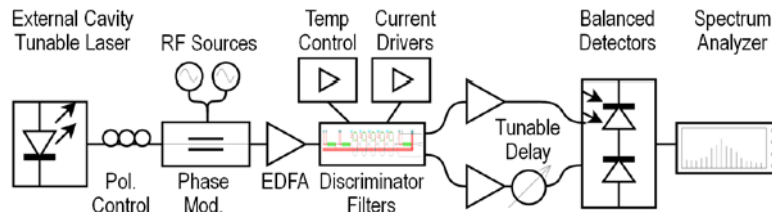


Fig. 3. Diagram of the system used for characterization.

4. Link results

4.1 Phase-modulated link with FIR filter

We performed link measurements using the FIR filter and phase modulation. Figure 4(a) illustrates the chip layout of two complementary sixth-order FIR filters with integrated 3dB splitter and polarization control. One of the filters was tuned to the desired linear ramp and linear phase transfer function. The phase and amplitude of the filter were measured with an optical vector network analyzer (OVNA) device and are shown in Fig. 4(b). The transfer function shown is normalized to a 7dB filter insertion loss. At the 50% field amplitude transmission point, both the amplitude and phase of the transfer function appear linear.

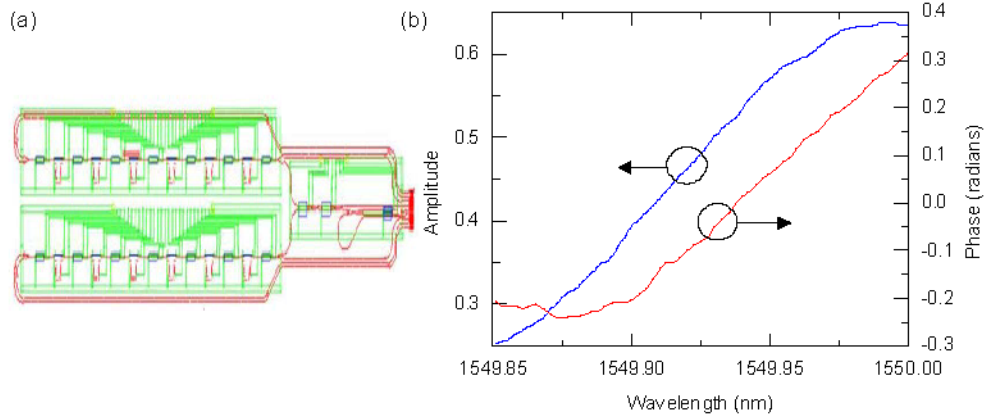


Fig. 4. (a) Layout of FIR filter chip. (b) Achieved filter amplitude and phase.

We report distortion measurements made with a single branch of the filter and single-ended detection. This is sufficient to determine whether the system can improve upon the third-order distortion over the MZM. With tones 2 GHz and 2 GHz + 100 kHz fundamental frequencies, we stepped the wavelength of the laser to determine the optimal bias point on the filter. At each wavelength, we collected the receiver power at 2 GHz and the third-order intermodulation distortion (IMD3) power at 2 GHz - 100 kHz. The result is shown in Fig. 5(a). At the optimal bias wavelength, we stepped the modulation power to demonstrate the distortion was cubic in power. The data is plotted in Fig. 5(b). The OIP3 was improved 6.7 dB better than a Mach Zehnder with the same received photocurrent.

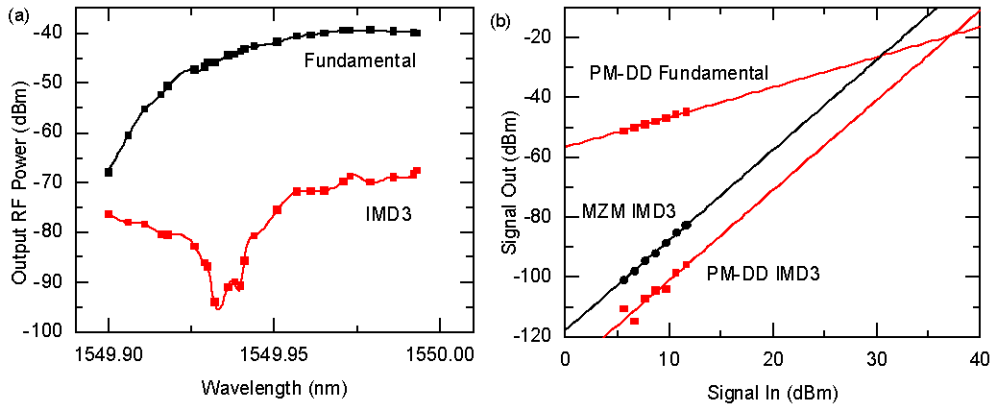


Fig. 5. (a) Fundamental and third-order intermodulation distortion versus laser wavelength. The modulation power is fixed at 10 dBm and the photocurrent is fixed at 0.11 mA. (b) Fundamental and third-order intermodulation distortion versus modulation power. The photocurrent is fixed at 0.11 mA and the wavelength is fixed at 1549.93 nm.

4.2 Phase-modulated link with IIR filter

We also performed PM-DD measurements with the IIR filter. Figure 6 shows the layout and tuned transfer function of one of the branches of the RAMZI filter. The plotted transfer function is normalized to 5 dB insertion loss. The transfer function was measured with an OVNA. The second branch was tuned to a transfer function with opposite slope.

For our first distortion measurement, we use fundamental frequencies of 5 GHz and 5 GHz + 100 kHz. Like with the FIR filter, we stepped the wavelength of the tunable laser and measured the fundamental and IMD3, but in this case, the measurement is performed with the balanced detection and two filters. The optical power is amplified so that the total DC photocurrent added from the two detectors is 10.5 mA. Figure 7(a) shows the calculated OIP3 from the fundamental and IMD3 data. Also shown on the graph is the theoretical OIP3 from a dual-output MZM with the same DC photocurrent, which we exceed for a range of biases.

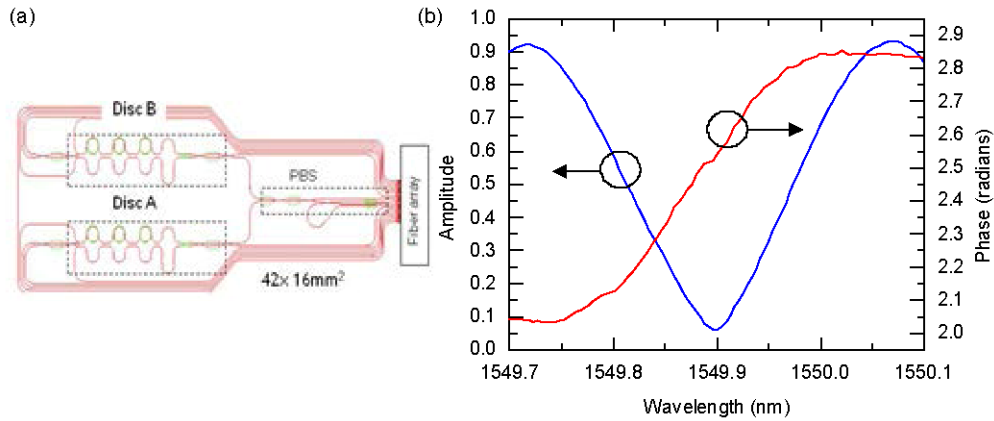


Fig. 6. (a) Layout of IIR filter chip. (b) Achieved filter amplitude and phase.

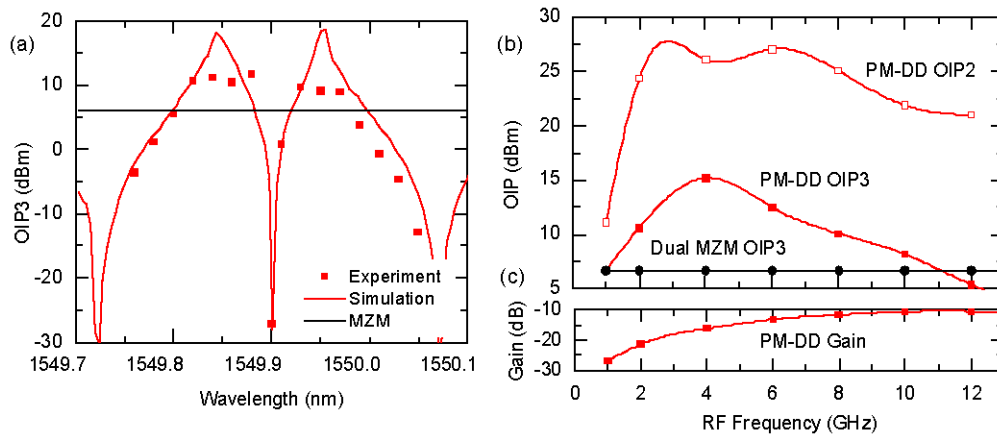


Fig. 7. (a) Output intercept point of third-order intermodulation distortion versus laser wavelength in simulation and experiment. The total photocurrent is fixed at 10.5 mA and the modulation frequency is 5 GHz. The theoretical OIP3 of a link with a dual-output MZM at the same received photocurrent is also plotted in the figure. (b) OIP3 and OIP2 versus modulation frequency at a fixed photocurrent of 10.5 mA and wavelength of 1549.964 nm. (c) Link gain.

Furthermore, the measured OVNA transfer function was used in a numerical link simulation, as described in [14]. The simulation trend of OIP3 versus wavelength matched with the experimental data, except for peaks around the optimal bias points. This may be due to optical system factors that are not included in the simulation, such as balancing the two

filters, fiber dispersion, polarization drift, back reflections, etc., or may be due to lack of resolution of the OVNA in measuring ripples in the transfer function.

We tuned the wavelength to 1549.964 nm, which is approximately 50% field transmission bias and around the maximum measured OIP3 at 5 GHz. Varying the modulation frequency, we measured both the IMD3 and the second harmonics, and calculated OIP3 and OIP2, shown in Fig. 7(b). For frequencies between 1 to 10 GHz, we exceed the OIP3 of the MZM. The best frequency was around 4 GHz, which gave us an 8.5 dB OIP3 improvement over the dual-output Mach-Zehnder. Because it is a balanced device, the second-order distortion is also low over the whole band. OIP2 and OIP3 should not be directly compared, however, since the theoretical value of OIP2 for the MZM is infinite if biased correctly. Our system will limit the dynamic range for a link with multi-octave bandwidth depending on the system noise and bandwidth. As seen in Fig. 7(c), the link gain increases for higher frequencies because of the 1/f PM to FM correspondence.

We compared the PM link and a dual-output MZM link using a high-power balanced photodetector array in development [15] to demonstrate the compression and output power characteristics of the link. The intended application is the delivery of high-power signals to remote transmission antennas. We expect the curves to be similar, but scaled down proportionally, with lower photocurrent. In both links, the signal gain falls off for large input signals as the nonlinear signal products capture more of the power, and the link eventually enters its nonlinear regime. As shown in Fig. 8(a), the PM-DD link achieved 4.3dB better RF compression power than the dual MZM. The link is nearly transparent, with only 3.8 dB signal loss. High enough input powers are plotted for the MZM link to show the regime where the linear approximation fails for the 1st order Bessel function term of the output signal expansion, and the output signal power oscillates with increasing input signal power. We expect the PM link to demonstrate a similar non-linear regime for higher input powers. As shown in Fig. 8(b), increasing the effective photocurrent, we achieved a maximum OIP3 of 39.2 dBm at 4GHz modulation frequency.

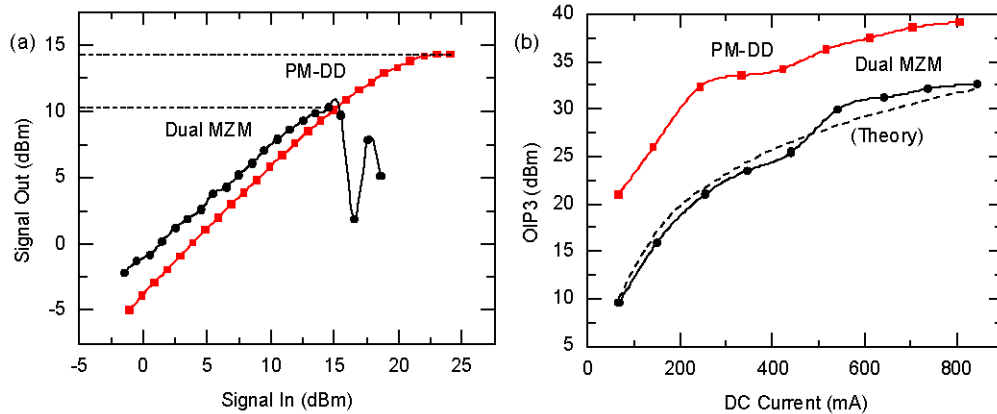


Fig. 8. (a) Output power versus modulation power compared to a dual-output Mach-Zehnder modulator measured experimentally. The frequency is fixed at 3.3 GHz and the effective DC photocurrent at 141 mA. (b) OIP3 versus effective DC photocurrent. The frequency is fixed at 4.0 GHz, and the modulation power is 0 dBm.

4.3 Frequency-modulated link with IIR filter

The FM laser we had available for our experiments was a distributed Bragg reflector laser designed by Bell Laboratories and fabricated by Multiplex Inc. It has a 45 kHz linewidth and 7.5 GHz / mA modulation efficiency at 100 MHz modulating the phase section of the device. The device was used in conjunction with the IIR discriminator to form an FM-DD link. Figure 9(a) shows the gain of the link compared to the PM-DD link. For a fairly small photocurrent of 5.2 mA per detector (10.5 mA total photocurrent), we are able to achieve

positive link gain for the FM-DD link for frequencies up to 500 MHz. Although the modulation efficiency falls off fairly fast because the device is operated by current injection, the link gain exceeds the lithium niobate phase modulator up past 3 GHz.

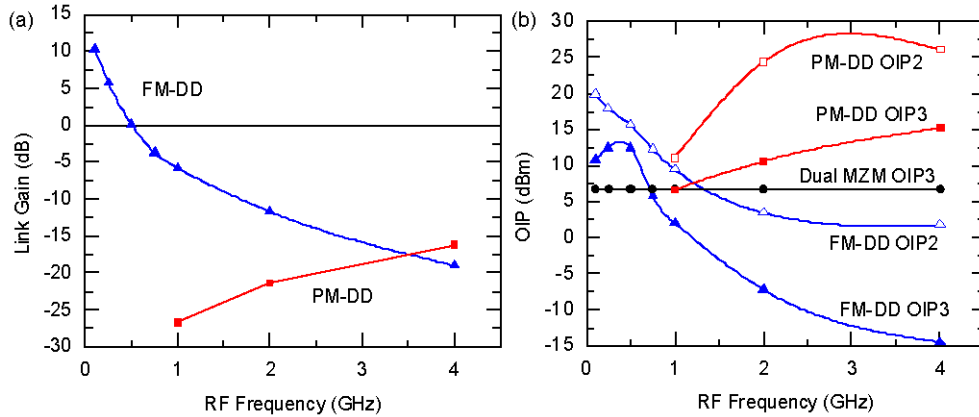


Fig. 9. (a) Link gain versus modulation frequency for the FM link versus the PM + IIR link. (b) Distortion versus modulation frequency, compared to the results of the PM + IIR link.

We measured the distortion of the link and compare it to the PM-DD and IMDD. Figure 9(b) compares OIP2 and OIP3 of the FM link with PM link data shown previously in Fig. 7. At its most linear frequency the FM laser exceeds the OIP3 of the Mach Zehnder by 5.8 dB, and the link has low second order distortion. The link gain and OIP3 degrade for higher modulation frequencies, but have significant improvements over IMDD and PM-DD links at low frequencies for both linearity and gain.

5. Conclusions

We have demonstrated phase-modulated and frequency-modulated microwave photonic links using complementary linear-field optical discriminators that greatly improve third-order link-linearity over traditional IMDD links, while maintaining low second-harmonic distortion through balanced detection. A phase modulated link with an FIR filter at 2 GHz modulation frequency had a 6.7 dB higher OIP3 than a MZM at the same photocurrent, but OIP2 was not measured. A phase modulated link with an IIR filter exceeded the OIP3 of an MZM for frequencies between 1 and 10 GHz, with an 8.5 dB OIP3 improvement over the MZM at 4 GHz. The OIP2 was greater than 26 dBm at 4 GHz, which is less than the theoretically infinite OIP2 of a quadrature biased MZM, but still large. An FM link with an IIR filter exceeded the OIP3 of an MZM for frequencies from 100 to 750 MHz, exceeding the OIP3 of the Mach Zehnder by 5.8 dB at 750 MHz modulation frequency, with an OIP2 of 16 dBm.

The system is not dependent on high-speed electronics for linearization, so it is scalable to higher microwave frequencies. With higher-order filter designs, such as discussed in [14], and further refinement, this type of discriminator may be able to achieve even much higher link linearity. We demonstrated link gain and good linearity for a low-frequency FM-DD link. Voltage modulated FM-laser devices that have wider bandwidths, such as devices using the quantum confined Stark effect, could be used as modulators in conjunction with our optical discriminators, in order to achieve high-gain, wide-bandwidth, linear FM-DD links.

Acknowledgments

This material is based upon work funded by DARPA's TROPHY program, under AFRL Contract No. FA8650-10-C-7003. Any opinions, findings and conclusions or recommendations expressed in this material are those of the authors and do not necessarily reflect the views of DARPA or the United States Air Force.